Available online at www.sciencedirect.com
ScienceDirect
Journal of Power Sources 165 (2007) 646–650
JOURNAL OF POWER SOURCES
www.elsevier.com/locate/jpowsour

Short communication

Improving electrochemical properties of lithium iron phosphate by addition of vanadium

Mu-Rong Yang *, Wei-hsin Ke, She-huang Wu

Department of Materials Engineering, Tatung University, 40 Chungshan N. Rd, Sec.3, Taipei 104, Taiwan

Available online 28 November 2006

Abstract

The poor conductivity, resulting from the low lithium-ion diffusion rate and low electronic conductivity in the $LiFePO_4$ phase, has posed a bottleneck for commercial applications. Well-crystallized $LiFePO_4$-based powders with vanadium addition were synthesized with solution method. The synthesized powders are coated with carbon. The powder containing the well-mixed $LiFePO_4$ and $Li_3V_2(PO_4)_3$ phases (LFVP) with narrow distributed particle size ranging between 0.5 and 2.5 μm exhibits improved electrochemical performance. The small particle size and the presence of the electronically conductive mixed phases can be the reasons why the cells containing LFVP exhibit the high discharge capacity of about 100 mAh g^{-1} at 10 C, whereas the samples with single phase, such as $LiFePO_4$ and $Li_3V_2(PO_4)_3$, have the discharge capacity less than 80 Ah g^{-1} at the same rate.

Keywords: Lithium iron phosphate; Cathode material; Vanadium

1. Introduction

Among the several materials under development for use as cathodes in lithium ion secondary batteries, lithium iron phosphate $LiFePO_4$ has been recognized as a promising candidate as material for cathode of Li-batteries due to the low cost, environmental benignity, cycling stability, and high theoretical capacity of 170 Ah g^{-1} [1,2]. However, the poor conductivity, resulting from the low lithium-ion diffusion rate and low electronic conductivity in the $LiFePO_4$ phase, has posed a bottleneck for commercial applications. Improvements in the conductivity have been achieved by two ways. One is to synthesize small and monodispersed particles [3–8] with electronically conductive coatings on powdered materials [9,10]; the other is to dope some elements to improve conductivity [11,12] and promote redox potential [13,14].

According to our knowledge, $LiFePO_4$ is prone to oxidation to produce $Li_3Fe_2(PO_4)_3$ or $LiFeP_2O_7$ during sintering. The existence of the $Li_3Fe_2(PO_4)_3$ or $LiFeP_2O_7$ in $LiFePO_4$ powders does little effect on the cycle life, although they will reduce the redox potential from 3.4 V (pure olivine phase) to 2.8 V ($Li_3Fe_2(PO_4)_3$) or 2.9 V ($LiFeP_2O_7$) versus Li/Li^+, respectively [2]. Patoux et al. reported $Li_3Fe_2(PO_4)_3$ and $Li_3V_2(PO_4)_3$ have the same crystal structures and space group. $Li_3V_2(PO_4)_3$ exhibited three redox plateaus around 3.59, 3.67, and 4.06 V [15–18]. Hence the higher redox potential will be expected if $Li_3Fe_2(PO_4)_3$ was substituted with $Li_3V_2(PO_4)_3$. In order to enhance the power density, the vanadium addition and a novel synthesis method will be employed in this study. Preliminary results indicate that the vanadium addition cannot only promote redox potential, which will facilitate the discharge capacity at high C rate.

2. Experimental

2.1. Synthesis procedures

The $LiFePO_4$-based were prepared with a solution method described in our previous report with oxidation of iron powder in aqueous solution of nitrates and phosphates [3]. V_2O_5 was used as the source of vanadium substitution. The precursor mixtures were atomized and formed into powders by the spray-dry method. These mixed powders were subsequently calcined at 750 °C for 6 h in nitrogen atmosphere and resulted in $LiFePO_4$-based powders.

* Corresponding author. Tel.: +886 2 25922458; fax: +886 2 25936897.
E-mail address: mryang@ttu.edu.tw (M.-R. Yang).

0378-7753/$ – see front matter © 2006 Elsevier B.V. All rights reserved.
doi:10.1016/j.jpowsour.2006.10.054

2.2. Structural and morphological characterizations

The crystalline structures of the prepared $LiFePO_4$ powders were measured with a SHIMADZU XRD-6000 diffractometer (Cu Kα radiation at 40 KV, 30 mA). The morphologies and particle size distribution can be observed by SEM (Hitachi S-800) equipped with energy dispersive spectrometry (EDS). EDS and elemental mapping were used to clarify the existence and distribution of vanadium and iron. The amount of C, N and H was determined by using an elemental analyzer (HERAEUS VarioEL-III for CNH). The particle size distribution was quantitatively determined by the optical particle size analyzer (Beckman Coulter LS 13 320).

2.3. Electrochemical characterization

The electrochemical properties of the synthesized powders were investigated in an electrochemical cell that comprised a cathode, and lithium metal anode and an electrolyte of 1 M $LiPF_6$ in EC (ethylene carbonate)-DEC (diethylene carbonate) solution. The cathode slurry was prepared by mixing synthesized powders with 10 wt.% carbon black and 7 wt.% polyvinylidene fluoride (PVDF) in *n*-methyl-2 pyrrolidone (NMP) solution. Since the thinner electrode can improve the electronic conductivity of the discharge capacity at high C rate [22], the tape-cast slurry on aluminum foil was carried out at gap heights of 100 μm. The thicker coating in this study can avert the improvement of the discharge capacity at high C rate contributed from the thickness reduction of the electrode, instead of from the modification of cathode materials. The cathode electrodes were roll-pressed after 110 °C × 8 h vacuum drying. All the cell's manipulations were made in an argon-filled glove box with oxygen and moisture of less than 2 ppm. The coin cells were galvanostatically charged and discharged over a voltage range of 2.5–4.3 V at different C rates in a multi-channel battery tester. The T-cell for cyclic voltammetry (CV) test was a three-electrode system [23]. The active materials were acted as working electrode and Li metal foils as the counter electrode and reference electrode. The electrochemical response was measured on a Solartron 1287 with voltage between 2.5 and 4.3 V at a scanning rate of 0.05 mV s^{-1}. The electronic conductivity of the synthesized powder was determined according to the method proposed by Celzard et al. [19].

3. Results and discussion

3.1. Crystalline structure analysis

The X-ray diffraction (XRD) patterns for the synthesized powders with various vanadium additions (x in molar fraction) in the $LiFePO_4$ samples (LFP for $x = 0$; LFVP for $x = 0.5$; LVP for $x = 1$) prepared in the nitrogen atmosphere at 750 °C are shown in Fig. 1. These sharp peaks in the patterns indicate that the powders are well crystalline. For the precursors with $x = 0$ and $x = 1$, the pure $LiFePO_4$ phase and pure $Li_3V_2(PO_4)_3$ phase can be obtained, respectively. The patterns are consistent with the JCPDS date and literature reports [16,17]. For the precursor

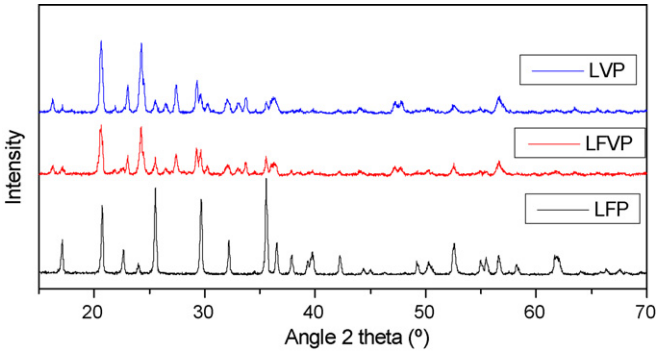

Fig. 1. X-ray diffraction patterns of the synthesized LFVP, LFP and LVP powders.

with $x = 0.5$ (LFVP), the synthesized powders are composed of $LiFePO_4$ and $Li_3V_2(PO_4)_3$ phases.

3.2. Microstructure of the powders

Scanning electron micrographs of $LiFePO_4/Li_3V_2(PO_4)_3$ compound materials (LFVP) sample are shown in Fig. 2. The particle size of sample ranged from 0.5 to 2.5 μm and exhibited a narrow distribution. From the EDS analysis and the elemental mappings of FeKα and VKα, they indicate that the $LiFePO_4$ and $Li_3V_2(PO_4)_3$ phases in LFVP were well dispersed and mixed. Hence it can be concluded that a powder (LFVP) of the well mixed $LiFePO_4$ and $Li_3V_2(PO_4)_3$ phases with carbon coating can be obtained.

3.3. Powder characterization

Table 1 shows the particle size distribution, carbon amounts and electronic conductivity of prepared samples. For the powder with single phase, such as LFP and LVP, the coalescence will lead to the grain growth. For LFVP, the grain growth is impeded by the presence of other phases. Hence, it is reasonable that LFVP of duplex phases had smaller particle size than LFP and LVP.

The small quantity of carbon coating (carbon content about 3.3%) can substantially enhance the electronic conductivity of $LiFePO_4$ powder. Due to the aqueous precursor, the synthesized particle can be uniformly covered with carbon to promote the electronic conductivity by small quantity of carbon coating [20,21]. For LFP, LFVP, and LVP with the similar carbon amount, as illustrated in Table 1, their conductivities are quite different. Among these three samples, the highest conductivity of LFVP may mainly be attributed to the smaller size of particle,

Table 1
Carbon contents, electronic conductivity and particle size of prepared samples

Sample	Carbon contents wt%	Electronic conductivity (Scm^{-1})	Particle size D_{50} (μm)
Pure of $LiFePO_4$	–	3.63×10^{-8}	8.44
LFP	3.31	6.75×10^{-3}	3.769
LFVP	3.52	2.5×10^{-2}	3.123
LVP	3.18	2.88×10^{-4}	4.037

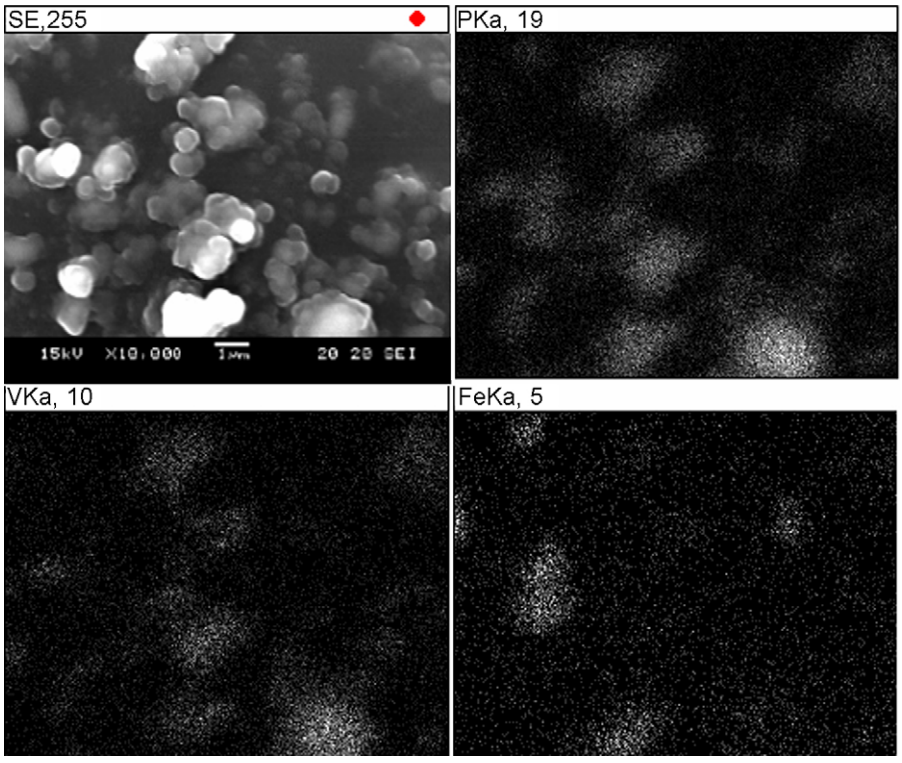

Fig. 2. (a) SEM of $LiFePO_4/Li_3V_2(PO_4)_3$/C compound sample (LFVP); (b) elemental mapping for P; (c) elemental mapping for V; (d) elemental mapping for Fe.

since the particles with smaller size will provide more contacts between particles.

3.4. Electrochemical performance

The cyclic voltammetry for the $LiFe_{0.5}V_{0.5}PO_4$ is shown in Fig. 3. It shows that the oxidation and reduction peaks appear in the way of the superimposition of the peaks of $LiFePO_4$ and $Li_3V_2(PO_4)_3$. No other peaks can be found. Oxidation peaks around 3.6, 3.7, and 4.1 V/Li can be ascribed to the oxidation of $Li_3V_2(PO_4)_3$; oxidation peak around 3.5 can be associated with the oxidation of Fe(II). Moreover, the peaks of the Fe(II)/Fe(III) redox potential are almost the same for all considered samples. Since $Li_xV_2(PO_4)_3$ exhibits an ordered Li phase at $x = 1$, 2, and 2.5, the plateaus around 3.6, 3.7, and 4.1 V can correspond to lithium extraction associated with the V^{3+}/V^{4+} redox couple, respectively [16–18]. Hence it can be concluded that the introduction of large amount of vanadium can lead to formation of more conductive phase, $Li_3V_2(PO_4)_3$. The duplex phase ($LiFePO_4$ and more conductive $Li_3V_2(PO_4)_3$ phases) will not only impede the grain growth during sintering, but also give the particles more electronically conductive. That will be beneficial to the electrochemical performance at high C rate. From the absence of the peak shift of the Fe(II)/Fe(III) redox potential, the vanadium doping effect in $LiFePO_4$ seems to play a minor role in this study of large amount of vanadium addition.

The cycle life of LFVP sample at the different C rates to a cut-off voltage between 2.5 and 4.3 V is shown in Fig. 4. For the early stage of charging/discharging test under the C/10 − 10 C rate, although the LFP sample exhibits high specific capacity

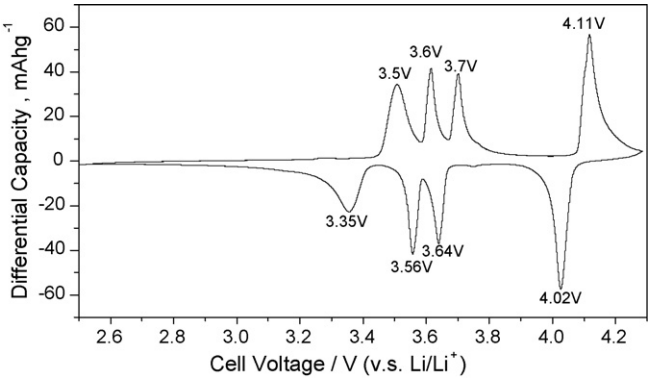

Fig. 3. CV of a V-added $LiFePO_4$ electrode in a EC-DEC (1:1) electrolyte cell with Li counter and reference electrodes, carried out at room temperature with the scan rate of 0.05 mV s^{-1}.

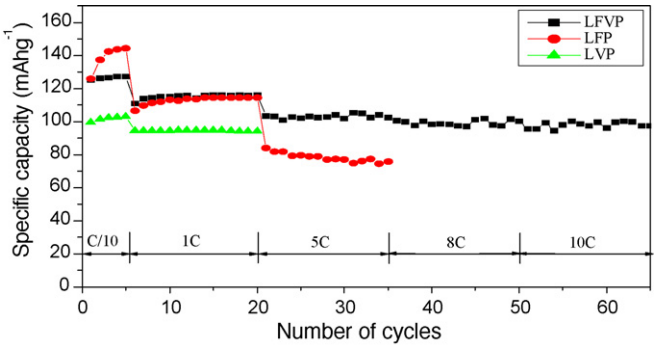

Fig. 4. Cycle performance of the synthesized LFVP, LFP and LVP samples under different C rates.

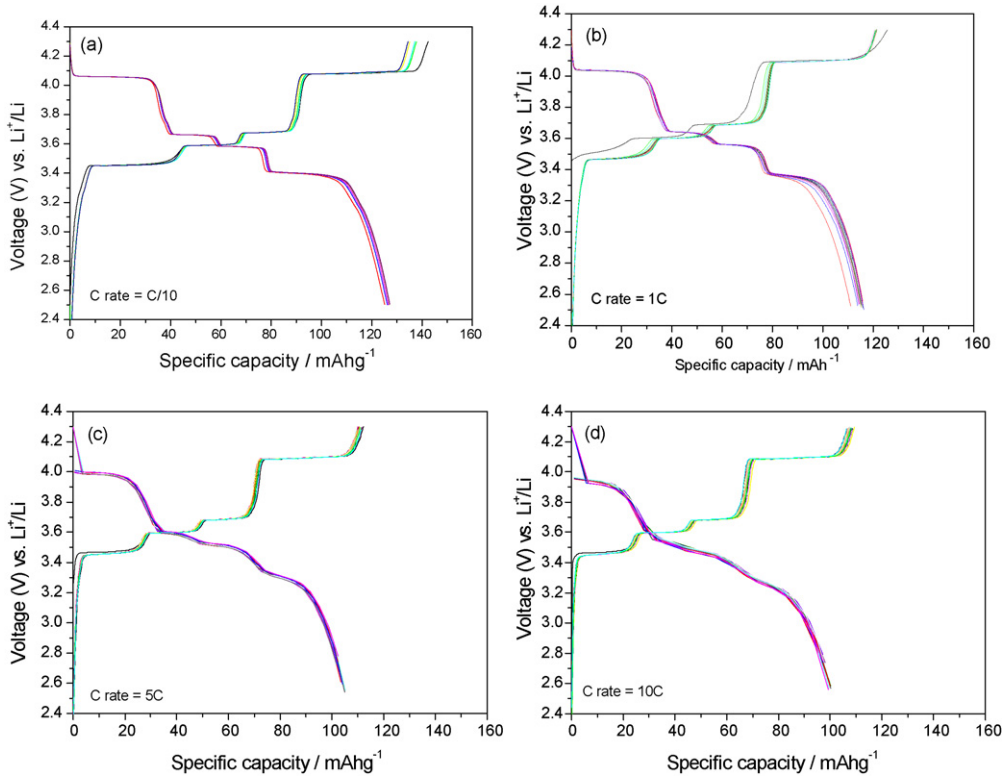

Fig. 5. Charge and discharge curves of $LiFePO_4/Li_3V_2(PO_4)_3$/C compound sample (LFVP). Charging was carried out at 0.5 C and discharging at 1–10 C.

than other samples under C/10 rate, the LFVP sample exhibits higher discharge capacity and lower fading rate at high C rate (5 C–10 C). At the high C rate, the discharge capacity at 10 C is about 77% of its maximum capacity, about 100 Ah g^{-1}. For the cells containing the sample with single phase, such as $LiFePO_4$ and $Li_3V_2(PO_4)_3$, the discharge capacity at 10 C is less than 80 Ah g^{-1}. The charge-discharge profiles for various discharging rates are shown in Fig. 5. Regardless of the scanning (discharging) rates in this study, the plateaus occur almost at the same voltage. The higher scanning rate (C rate), the higher slope around discharge plateaus is, as expected. It can be concluded that the redox mechanisms seem to remain the same, that is, the redox mechanisms are independent of discharging rate.

4. Conclusions

Well-crystallized powders of $LiFePO_4$ based powder with vanadium addition can be synthesized from mixture of iron powder and the aqueous solution containing H_3PO_4, LiOH, citric acid and polyvinyl acetate. The pure $LiFePO_4$ powder, pure $Li_3V_2(PO_4)_3$ powder and the powders (LFVP) composed of $LiFePO_4$ and $Li_3V_2(PO_4)_3$ phases are coated with carbon. The cells containing LFVP as cathode exhibit highest discharging capacity at 10 C. This can be attributed to the smallest particles among three samples as well as the presence of the carbon coating and the electronically conductive $Li_3V_2(PO_4)_3$ phase. However, for the cells containing samples with single phase, such as $LiFePO_4$ and $Li_3V_2(PO_4)_3$, the discharge capacity of 10 C is less than 80 Ah g^{-1}.

Acknowledgements

The authors are indebted to the financial support of Tatung Company.

References

[1] A.K. Padhi, K.S. Nanjundaswamy, J.B. Goodenough, J. Electrochem. Soc. 144 (4) (1997) 1188–1194.
[2] A.K. Padhi, K.S. Nanjundaswamy, C. Masquelier, Okada, J.B. Goodenough, J. Electrochem. Soc. 144 (5) (1997) 1609–1613.
[3] S.H. Wu, K.M. Hsiao, W.R. Liu, J. Power Sources 146 (2005) 550–554.
[4] M.R. Yang, W.H. Ke, S.H. Wu, J. Power Sources 146 (2005) 539–543.
[5] S. Franger, F. Le Cras, C. Bourbon, H. Roualt, Electrochem. Solid-state Lett. 5 (10) (2002) A231–A233.
[6] G. Arnold, J. Garche, R. Hemmer, S. Strobele, C. Vogler, M. Wohlfahrt-Mehrens, J. Power Sources 119–121 (2003) 247–251.
[7] T.H. Cho, H.T. Chung, J. Power Sources 133 (2004) 272–276.
[8] K.F. Hsu, S.Y. Tsay, B.J. Hwang, J. Mater. Chem. 14 (2004) 2690–2695.
[9] F. Croce, A. D' Epifanio, J. Hassoun, A. Deptula, T. Olczac, B. Scrosati, Electrochem. Solid-state Lett. 5 (3) (2002) A47–A50.
[10] Z. Chen, J.R. Dahn, J. Electrochem. Soc. 149 (9) (2002) A1184–A1189.
[11] S.Y. Chung, Jasont Bloking, Y.M. Chiang, Nat. Mater. 1 (October) (2002) 123–128.
[12] G.X. Wang, Steve Bewlay, Jane Yao, J.H. Ahn, S.X. Dou, H.K. Liu, Electrochem. Solid-state Lett. 7 (12) (2002) A503–A506.
[13] Atsuo Yamada, S.C. Chung, J. Electrochem. Soc. 148 (8) (2001) A960–A967.
[14] N. Penazzi, M. Arrabito, M. Piana, S. Bodardo, S. Panero, I. Amadei, J. Eur. Ceram. Soc. 24 (2004) 1381–1384.
[15] Sebastien Patoux, Calin Wurm, Mathieu Morcrette, Gwenaelle Rousse, Christian Masquelier, J. Power Sources 119–121 (2003) 278–284.
[16] H. Huang, S.C. Yin, Tracy Kerr, Nicholas Taylor, Linda F. Nazar, Adv. Mater. 14 (21) (2002) 1525–1528.

[17] M.Y. Saidi, J. Barker, H. Huang, J.L. Swoyer, G. Adamson, J. Power Sources 119–121 (2003) 266–272.
[18] J. Barker, M.Y. Saidi, J.L. Swoyer, J. Electrochem. Soc. 150 (6) (2003) A684–A688.
[19] A. Celzard, J.F. Mareche, F. Payot, G. Furdin, Carbon 40 (15) (2002) 2801–2815.
[20] Z. Chen, J.R. Dahn, J. Electrochem. Soc. 149 (9) (2002) A1184–A1189.
[21] R. Dominko, M. Gaberscek, J. Drofenik, M. Bele, S. Pejovnik, J. Jamnik, J. Power Sources 119–121 (2003) 770–773.
[22] Denis Y.W. Yu, Kazunori Donoue, Takao Inoue, Masahisa Fujimoto, Shin Fujitani, J. Electrochem. Soc. 153 (5) (2006) A835–A839.
[23] M.G.S.R. Thomas, P.G. Bruce, J.B. Goodenough, Solid State Ionics 18–19 (1986) 794–798.